www.czasopisma.pan.pl www.journals.pan.pl
Chemical and Process Engineering 2015, 36 (1), 73-87
DOI: 10.1515/cpe-2015-0006

# A MODIFIED GIBBS FREE ENERGY MINIMISATION MODEL FOR FLUID BED COAL GASIFICATION

Marek Ściążko, Leszek Stępień *

AGH University of Science and Technology, 30 Mickiewicza Av., 30-0589 Cracow, Poland

A modified approach to equilibrium modelling of coal gasification is presented, based on global thermodynamic analysis of both homogeneous and heterogeneous reactions occurring during a gasification process conducted in a circulating fluid bed reactor. The model is based on large-scale experiments (ca. 200 kg/h) with air used as a gasification agent and introduces empirical modifications governing the quasi-equilibrium state of two reactions: water-gas shift and Boudouard reaction. The model predicts the formation of the eight key gaseous species: CO, $CO_2$, $H_2O$, $H_2$, $H_2S$, $N_2$, COS and $CH_4$, volatile hydrocarbons represented by propane and benzene, tar represented by naphthalene, and char containing the five elements C, H, O, N, S and inorganic matter.

**Keywords:** equilibrium modelling, coal gasification, gasification modelling, fluid bed gasification

## 1. INTRODUCTION

One of the alternative technologies to conventional coal combustion is gasification, which makes it possible to produce a combustible gas that might be used in an integrated gasification combined cycle (IGCC) to produce electrical power with high efficiency, or which, after upgrading to syngas, can be used for chemical synthesis. Gasification also enables the conversion of almost every carbonaceous material to syngas, including the processing of biomass and wastes as well as high- and low-quality coal. The gasification process requires the delivery of a particular quantity of oxygen that enables partial fuel combustion, necessary to generate the energy needed to balance endothermic gasification reactions. The composition of the generated syngas strongly depends on the composition of gasification blast and process conditions, but in all cases the main gaseous products are carbon monoxide, carbon dioxide, hydrogen, and methane. Additionally, some minor components of syngas are present, such as higher hydrocarbons and compounds containing sulphur (hydrogen sulphide) or nitrogen (ammonia), in quantities very much dependent on the applied gasification technology.

In a case of an air-blown gasifier, nitrogen will become one of the main components of the syngas, resulting in a low calorific gas suitable mainly for energy production. For other applications such as chemical synthesis, oxygen is used as the gasifying agent, in addition to steam in hydrogen production by gasification.

At present three types of gasification reactors are used in commercial applications – fixed beds, fluid beds and entrained gasifiers. Air gasification is usually performed in fluidised bed gasifiers, which operate in the temperature range of 1000–1300 K. The air used in this type of gasifier might be enriched with steam, which will increase hydrogen generation (Pengmei et al., 2007), resulting in a higher calorific value of the gas produced, and will help reduce the content of condensing light

*Corresponding author, e-mail: lstepien@agh.edu.pl

hydrocarbons and tar by increasing the progress of cracking of released volatiles. Due to the environmental aspects of fossil fuel conversion, more and more attention is being directed to the problem of gasification with carbon dioxide as a way to utilise $CO_2$, produced for instance during conventional combustion (Irfan, 2011). This process can be conducted only in fixed or fluid beds, in which char is available as a reducing agent, making the Boudouard reaction $C + CO_2 \rightarrow 2CO$ possible. In an entrained bed gasifier, high temperature and relatively low volume concentration of the reacting fuel do not create suitable conditions for this reaction.

Developing new technologies would be impossible without prior modelling and simulation of the process. In the case of gasification several different approaches to this problem might be used. Models range from the simplest, but also the least effective, stoichiometric models, through more complex equilibrium models, up to the most advanced and effective kinetic and CFD models.

Stoichiometric modelling is based on knowledge of the reactions that take place inside the gasifier, and its goal is to obtain the stoichiometric coefficients of the products based on the assumed or measured flow rate of the inlet streams, their composition, and a calculated mass balance. In gasification, a stoichiometric model might be presented in the form of Eq. (1) (Kaiho and Yamada, 2012; Rao et al., 2004):

$$C_x H_y O_z + \alpha \times \text{oxidant} \rightarrow \beta_i \times \text{product}_i \tag{1}$$

where α is the known amount of oxidant used in a gasification process, and $\beta_i$ are unknown coefficients to be determined by experimentation. A similar approach is used in equilibrium modelling, which needs particular reactions to be specified, although the final composition of products is calculated based not only on a mass balance equation but also on the values of equilibrium constants for specific reactions. Equilibrium models are especially useful for modelling entrained flow gasifiers, where the temperature reaches 1800 K (Rao et al. 2004) and the kinetics of chemical reactions can be neglected. In fluidised bed reactors a more general approach, also leading to finding the equilibrium composition, is needed. This is possible thanks to the free Gibbs energy minimisation method (Neron et al., 2012), sometimes called the Gibbs reactor method. The main advantage of this method, which is especially important in case of a complex multi-reaction process like gasification, is that there is no need to describe the mechanism of the process, only to specify the initial and final components. Equilibrium state is found by minimising of the total free Gibbs energy of the system, which gives the composition of the products. The most sophisticated and complete method of modelling chemical processes includes kinetics of reactions and preferably mass and heat transfer conditions. This is done with the use of CFD applications, which require a vast amount of input data as well as sufficient computing power. Nevertheless, at the present time this is the most widely used method of simulating gasification, and a number of publications can be found concerning CFD gasification. They cover different aspects of the problem, and may be focused on the modelling of a particular reactor type (moving bed (Mann et al., 2004), fluid bed (Jarungthammachote and Dutta, 2008; Miao et al., 2013) entrained (Chen et al., 2012; Silaen and Wang, 2010; Tremel and Spliethoff, 2013); on temperature distribution, flow properties or multiphase interactions (gas-solid). However, as mentioned above, even these complicated models are not perfect, because they still require many empirical parameters concerning quasi-equilibrium conditions, reaction kinetics, heat and mass transfer, or the dynamics of multiphase flows.

Calculating the equilibrium conditions of a gasification process might be difficult because of its complexity, which is a mixture of heterogeneous (gas-solid) and homogeneous (gas-gas) reactions. Despite this, a number of papers can be found discussing various ways of finding equilibria or quasi-equilibria of such processes. The Gibbs minimisation method was used by (Shabbar and Janajreh, 2013) who proposed to calculate the equilibrium composition using a very complex model, considering the formation of 44 species. They reported good accuracy as far as trends in changes of concentrations in temperature are concerned, but with a tendency to overestimate yields of CO compared with those reported in the literature. The same method was used by (Li et al., 2001) to find the equilibrium

composition in gasification, but application of their model to simulating fluid bed gasification did not produce good accuracy. They reported flaws in the thermodynamic approach to gasification due to kinetic effects and mass transfer phenomena, which are especially important in two-phase processes. (Florin and Harris, 2007) studied hydrogen production from biomass based on thermodynamic analysis of gasification process and they suggested different deviations from the equilibrium model: overprediction of carbon conversion, underestimation of $CH_4$, differences in tar yield and composition in comparison to experimental results and overestimation of $H_2$ concentration in the product gas. Some improvement to Gibbs energy minimisation method was proposed by (Esmaili et al., 2013), who introduced empirical temperature correction enabling calculation of the temperature of the equilibrium state, different to that given by thermodynamic calculations. A different approach is described in (Nguyen et al., 2010; Yoshida et al., 2008), who underline the problem of estimating carbon conversion in an equilibrium model. Both papers propose two-stage equilibrium modelling, treating gas-solid reactions in the first step, and gas-gas reactions in the second. This approach enables accurate assessment of the amount of carbon conversion and eliminates some problems concerning mass transfer limitations. Yoshida reports improvement in the accuracy of simulated data in comparison with the conventional equilibrium model. Another modification of the Gibbs minimisation method was reported by (Kangas et al., 2014) who present different cases of modification of thermodynamic equilibrium by introducing additional pre- or post-processing correlations for gas phase composition as well as the formation of char and tars.

Despite the above mentioned restrictions, equilibrium models are useful tools for basic process control, because of the ease of analysis of important gasification parameters. Considering the non-equilibrium paths of some reactions occurring during gasification, in this study, a modified approach to coal gasification is presented, based on global thermodynamic analysis of both homogeneous and heterogeneous reactions occurring during a gasification process conducted in a circulating fluid bed reactor and introducing empirical modifications governing their quasi-equilibrium state. Final gas composition is a result of combined effect of equilibrium gasification reactions and non-equilibrium pyrolysis. Considerations of both effects are provided in this work by means of a modified Gibbs energy function formulation. The model is based on large-scale experiments with air used as a gasification agent.

## 2. METHODOLOGY

### *2.1. The Gibbs energy minimisation method*

The following model is based on the free Gibbs energy minimisation method, which is convenient in the analysis of complex processes like gasification, because it does not require specification of separate reactions, but uses only the compositions of inlet and outlet streams. The essence of the method is to minimise the total Gibbs free energy of the substances present in the system at a given temperature and pressure. For better accuracy, the thermodynamic model was improved by adding some correction factors reflecting real, quasi-equilibrium states for two selected but leading reactions. The model predicts the formation of the eight key gaseous species: CO, $CO_2$, $H_2O$, $H_2$, $H_2S$, $N_2$, COS and $CH_4$, volatile hydrocarbons represented by propane and benzene, tar represented by naphthalene, and char containing five elements C, H, O, N, S and inorganic matter. For simplification purposes, mineral matter is treated as inert without pressure activity, which means that it influences only the energy balance of the process. The thermodynamic properties of ash were represented by $SiO_2$. In order to calculate the Gibbs total free energy function for the gas phase, Eq. (2) was defined in a Mathcad 15 environment.

$$G(T) = \sum_{i=1}^{8} n_i \Delta G_i(T) + RT \sum_{i=1}^{11} n_i \ln \frac{n_i}{\sum n_i} \tag{2}$$

Because the pressure inside the reactor is close to the atmospheric one, it was assumed that gas products can be treated as an ideal gas mixture. The indices in the first and second parts of this function are different because it was assumed that only eight gaseous species are the result of equilibrium state reactions, while propane, benzene representing light hydrocarbons, and naphthalene representing tar are the result of the non-equilibrium reaction of pyrolysis as a preliminary stage of the thermal decomposition of coal. The second part of this function corresponds to the effect of the mixing of gases and hydrocarbons produced during pyrolysis – devolatilisation of coal, so the presence of all gaseous compounds is necessary.

The change in Gibbs energy for each component is defined as a function of temperature by Eq. (3).

$$\Delta G_i(T) = \Delta H_i(T) - T\Delta S_i(T) \tag{3}$$

The molar enthalpy of each component was calculated by the standard formula (4):

$$\Delta H_i(T) = \Delta_f H_i + \int_{T_0}^{T} C_{pi}(T) dT \tag{4}$$

The molar entropy for each component was calculated from (5):

$$\Delta S_i(T) = \Delta S_i^0 + \int_{T_0}^{T} \frac{C_{pi}(T)}{T} dT \tag{5}$$

Molar heat capacity was given in the form of polynomials with coefficients *a, b, c, d, e* specified for each component (6) (Szarawara, 2007). The coefficients for Eq. (6) are presented in Appendix A:

$$C_p(T) = a + b \times 10^{-3} T + c \times 10^{-6} T^2 + \frac{d \times 10^5}{T^2} + e \times 10^{-9} T^3 \tag{6}$$

The model was developed for the case of air gasification. The quantities of air and coal introduced to the reactor in simulations were equal to those used in experiments. The experimental data were used to validate and improve the thermodynamic model. The composition of air included oxygen, nitrogen and moisture at 70% relative humidity.

To find the solution of Eq. (2), the minimisation problem was solved and restricting equations were introduced. For the thermodynamic model, five equations representing the molar balance for each element present in the system were used (7-11):

Carbon:

$$n_{C_{coal}} = n_{CO_2} + n_{CO} + n_{CH_4} + n_{COS} + n_{C_{char}} + 6n_{C_6H_6} + 8n_{C_8H_{10}} + 3n_{C_3H_8} \tag{7}$$

Hydrogen:

$$\begin{aligned} & n_{H_{coal}} + n_{H_2O_{coal}} + n_{H_2O_{air}} = \\ & = n_{H_2O} + 2n_{CH_4} + n_{H_2} + 5n_{C_8H_{10}} + 4n_{C_3H_8} + 3n_{C_6H_6} + n_{H_2S} + n_{H_{char}} \end{aligned} \tag{8}$$

Oxygen:

$$\begin{aligned} & n_{O_{coal}} + n_{O_2} + 0.5(n_{H_2O_{air}} + n_{H_2O_{coal}}) = \\ & = 0.5n_{H_2O} + n_{CO_2} + 0.5n_{CO} + 0.5n_{COS} + n_{O_{char}} \end{aligned} \tag{9}$$

Nitrogen:

$$n_{N_{coal}} + 3.76 n_{O_2} = n_{N_2} + n_{N_{char}} \tag{10}$$

Sulphur:

$$n_{S_{coal}} = n_{H_2S} + n_{COS} + n_{S_{char}} \tag{11}$$

Additionally, the energy balance (12) based on the enthalpies of the inlet and outlet streams was evaluated outside the main calculation block for each temperature. The reference temperature was equal to the standard one, 298 K, and therefore only the enthalpies of formation were used in the inlet streams. The mass specific enthalpy was used if the quantity of a substance was expressed in terms of mass (coal, char); otherwise molar enthalpy was taken.

$$\Delta h_{\text{coal}} + \Delta h_{\text{air}} = \Delta h_{\text{char}} + \Delta h_{\text{ash}} + \Delta h_{\text{gas}} + \Delta h_{\text{tar}} + \Delta \text{h}_{\text{CnHm}} + \Delta \text{h}_{\text{C6H6}} + Q \tag{12}$$

Heat loss $Q$ was considered to be constant and equal to 16 kW. This value was calculated based on the geometry and dimensions of the reactor shown in Fig. 1, taking into account its estimated surface and outer shell temperatures. The total enthalpy of a stream was calculated as a sum of the chemical and physical enthalpies of each species according to Eq. (13), with respect to molar enthalpies for gaseous and liquid products and specific enthalpies for coal and char. For pure species standard enthalpy of formation was taken from (Szarawara, 2007).

$$\Delta h_i = n_i[\Delta_f H_i + C_{pi}(T)(T - T_0)] \tag{13}$$

Specifically for coal and char, Eq. (14) was applied:

$$\Delta h_{\text{solid}} = m_{\text{solid}}[\Delta_f H_{\text{solid}} + C_{p\text{solid}}(T)(T - T_0)] + n_{\text{moisture}} \Delta h^{(l)}_{\text{H2O}} \tag{14}$$

The procedure used to calculate the enthalpy of coal and char formation is presented in the following section.

### *2.2. Enthalpy of coal and char formation*

The enthalpy of coal formation was calculated according to the algorithm presented by (Sciazko, 2013). The methodology is based on the fact that there exists a difference between the sum of the heats of combustion for the particular elements forming coal, and the coal's heat of combustion. The algorithm used to calculate the enthalpy of formation also includes a correction function based on the content of oxygen in the coal. Heat of combustion is calculated by the formula (15)

$$\Delta_C H_{\text{coal}} = -327.633 C^{daf} - 1417.892 H^{daf} - 92.768 S^{daf} \quad \text{[kJ/kg]} \tag{15}$$

The correction function is given by Eq. (16).

$$f(\theta) = 0.01379 \ln(\theta) - 0.01393 \theta^{0.75} + 1.02111 \tag{16}$$

Finally, the enthalpy of coal or char formation [kJ/kg] is given by Eq. (17).

$$\Delta_f H^{daf}_{\text{coal}} = \Delta_C H_{\text{coal}} \times [1 - f(\theta)] \quad \text{[kJ/kg]} \tag{17}$$

The method gives the value of enthalpy of formation for a dry ash-free basis, and must be referenced to the as-received (18) in order to be used in the energy balance equation.

$$\Delta_f H_{\text{coal}} = \Delta_f H^{daf}_{\text{coal}} \times (1 - A^r) \tag{18}$$

### *2.3. Experimental setup*

In order to develop a final model, a series of gasification test runs were performed. The experiment was conducted using a test plant with a capacity of 150–300 kg of coal per hour, as shown in Fig. 1. The plant consisted of a coal feeding system (1), circulating fluid bed (2), char separation cyclones and char hopper (3, 4, 5), and heat recuperation and gas cleaning systems. The reactor is composed of two zones, the bottom one with the diamter of 380 mm, and the riser with the height of 3640 mm.

Table 1. Average composition of coal used in experimental tests

| | $C^{ar}$ | $H^{ar}$ | $O^{ar}$ | $N^{ar}$ | $S^{ar}$ | $W^{t}$ | $A^{a}$ | $V^{a}$ |
|---|---|---|---|---|---|---|---|---|
| (wt. %) | 69.41 ±0.6 | 4.12 ±0.27 | 9.08 | 1.34 ±0.15 | 0.73 ±0.04 | 5.02 ±0.5 | 10.30 ±0.2 | 31.80 ±0.17 |

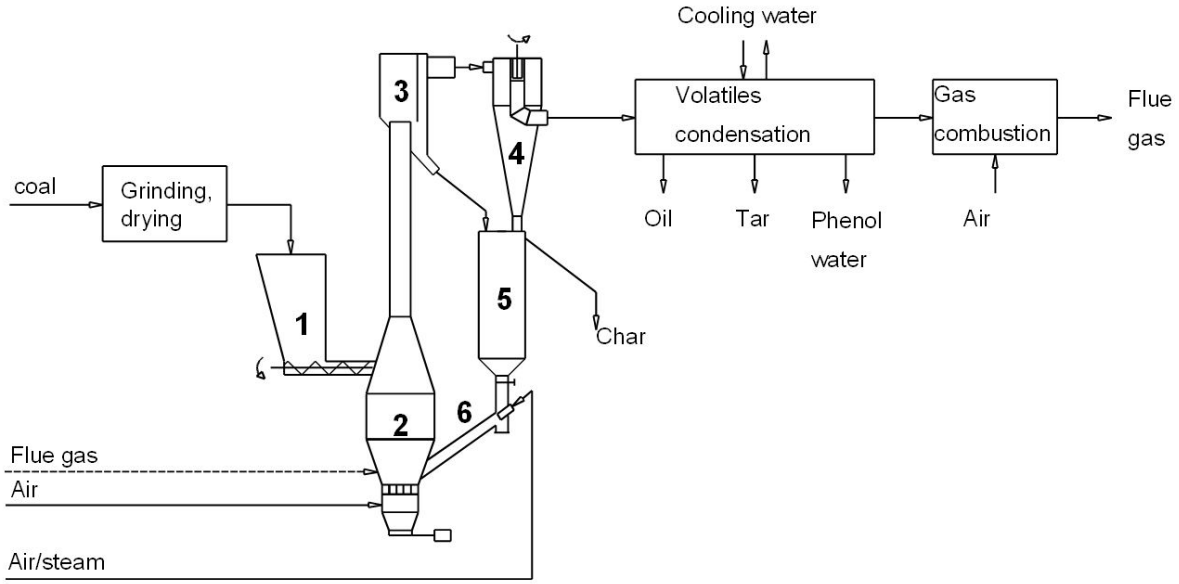


Fig. 1. Schematic diagram of the experimental setup

The experiment was performed on Polish bituminous coal from the Wieczorek mine, an analysis of which is presented in Table 1. Tests were run with different coal-to-air ratios, with the coal inlet stream varying between 180–300 kg/h and the air stream between 150–200 $Nm^3/h$. The air used in the experiment was preheated up to a temperature between 250-300°C. The results of experimental tests concerning the calorific value and $CO/CO_2$ ratio of the syngas are presented in Figs. 2A and 2B.

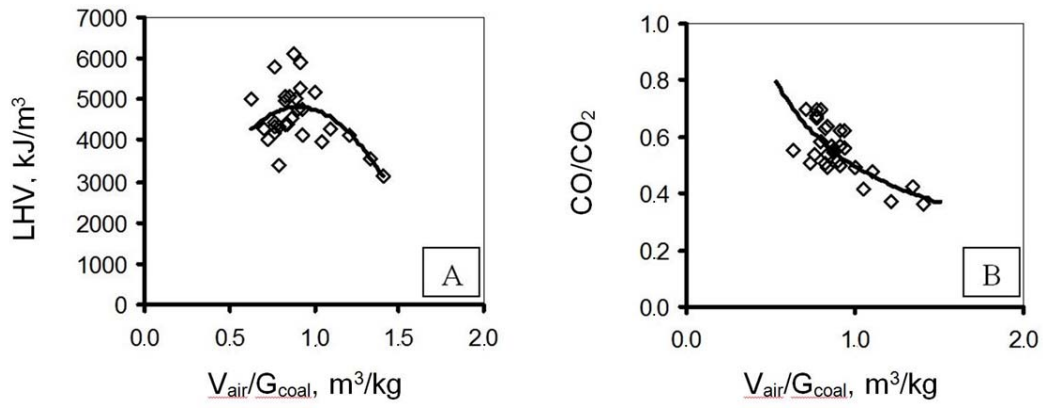


Fig. 2. Experimental results for the effect of the air-to-coal ratio on the calorific value (A) and CO-$CO_2$ ratio (B) of the gas

The experimental part of the study was finalised with an overall mass bass balance calculated by means of relative mass error given by Eq. (19)

$$\delta = \frac{\rho_{air} V_{air} + m_{coal} - m_{char} - \rho_{gas} V_{gas}}{\rho_{air} V_{air} + m_{coal}} \times 100\% \tag{19}$$

Gas density was calculated using the measured fractions of each component and their standard densities. The results are presented in Table (2). Ultimate analysis was performed using two different devices: LECO CHN628 and LECO 628S. Concentration of oxygen was calculated as a complement to 100%. Approximate analysis of coal and char was performed using LECO TGA 701 analyser. The amount of volatile matter was according to Polish standard PN-G-04516:1998.

The mass flow of coal and char were calculated knowing the mass of solid in the hopper over the screw conveyor used for transporting coal to the reactor and time spent to empty that volume. Streams of air and produced gas were measured with calibrated orifices. Measurement errors were estimated to be 1.5% for air, 8% for syngas due to the changes in composition which result in changes in density. The average error for coal stream did not exceed 5%. Gas composition was established using VARIAN CP3800-2004 chromatograph with two detector types, FID and TCD. Separate gas samples were taken in order to find benzene concentration. Gas was collected to wash bottles filled with isopropanol and then analysed in Thermo Scientific Trace GC Ultra gas chromatograph.

Table 2. Experimental results for a series of gasification runs

| | Experimental data | | | | | | Uncertainty |
|---|---|---|---|---|---|---|---|
| Air ($Nm^3/h$) | 200 | 179 | 178 | 198 | 150 | 170 | ±1.50% |
| Coal (kg/h) | 300 | 248 | 234 | 250 | 171 | 191 | ±5.00% |
| $V_{air}/G_{coal}$ ($m^3/kg$) | 0.667 | 0.716 | 0.766 | 0.792 | 0.882 | 0.916 | |
| Temperature (K) | 1160 | 1080 | 1170 | 1200 | 1190 | 1140 | ±2.50 |
| $N_2$ (%vol.) | 63.0 | 64.8 | 59.6 | 61.9 | 59.0 | 60.9 | ±0.98 |
| $H_2$ (%vol.) | 5.8 | 7.1 | 9.0 | 7.4 | 9.1 | 7.9 | ±0.43 |
| CO (%vol.) | 7.8 | 7.8 | 7.9 | 8.1 | 7.7 | 8.3 | ±0.13 |
| $CO_2$ (%vol.) | 15.4 | 13.4 | 15.5 | 14.9 | 13.9 | 14.7 | ±0.17 |
| $CH_4$ (%vol.) | 4.4 | 4.8 | 4.1 | 4.6 | 5.3 | 5.1 | ±0.10 |
| $C_6H_6$ (%vol.) | 0.7 | 0.7 | 0.7 | 0.7 | 0.7 | 0.7 | ±0.018 |
| $C_nH_m$(%vol.) | 1.6 | 1.6 | 1.6 | 1.6 | 1.6 | 1.6 | ±0.03 |
| Dry gas yield ($m^3/h$) | 249.5 | 218.2 | 235.9 | 252.7 | 200.8 | 234.1 | ±8.00% |
| Char yield (kg/h) | 161.0 | 128.0 | 110.0 | 145.0 | 89.0 | 105.0 | ±5.00% |
| δ (%) | 11.45 | 13.62 | 9.79 | 5.61 | 5.91 | 6.19 | |

Table 3. Average composition of char obtained in experimental tests

| | $C^{ar}$ | $H^{ar}$ | $O^{ar}$ | $N^{ar}$ | $S^{ar}$ | $W^{t}$ | $A^{a}$ | $V^{a}$ |
|---|---|---|---|---|---|---|---|---|
| (wt. %) | 75.65 ±0.6 | 0.97 ±0.27 | 0 | 1.28 ±0.15 | 0.62 ±0.04 | 1.00 ±0.5 | 20.48 ±0.2 | 3.28 ±0.09 |

In order to validate the performance of the thermodynamic model, six simulations were performed with exactly the same air and coal streams as in the experimental tests. The experimental parameters and test results are presented in Table 2. The concentration of $C_nH_m$ presented in the table represents the total amount of light hydrocarbons ($C_2H_4$-$C_3H_8$) measured during the experiment. $C_3H_8$ was the main

component of light hydrocarbons and was chosen as a model representative in Gibbs energy minimisation function. Properties of char obtained during the experimental test are presented in Table 3.

## 3. RESULTS AND DISCUSSION

In the first step of the calculations, Gibbs free energy minimisation was performed in a range of temperatures typical for fluidised bed gasification, as a result of which the composition of products was obtained as a function of temperature. Minimisation was performed in Mathcad 15 environment using the nonlinear conjugate gradient method to find the minimum of the function (2). The overall mass balance of the process was used as a closing equation. Then, using an iterative method, a temperature satisfying Eq. (12) was found. This temperature can be called the operation temperature, and it was interpreted as the temperature of a quasi-equilibrium state. Minimisation of the Gibbs free energy function produced results for the composition of gaseous species and tar compounds. Char composition was obtained from the difference between the initial number of moles of each element and their quantity in the gaseous products. The computational algorithm is presented in Fig. 3.

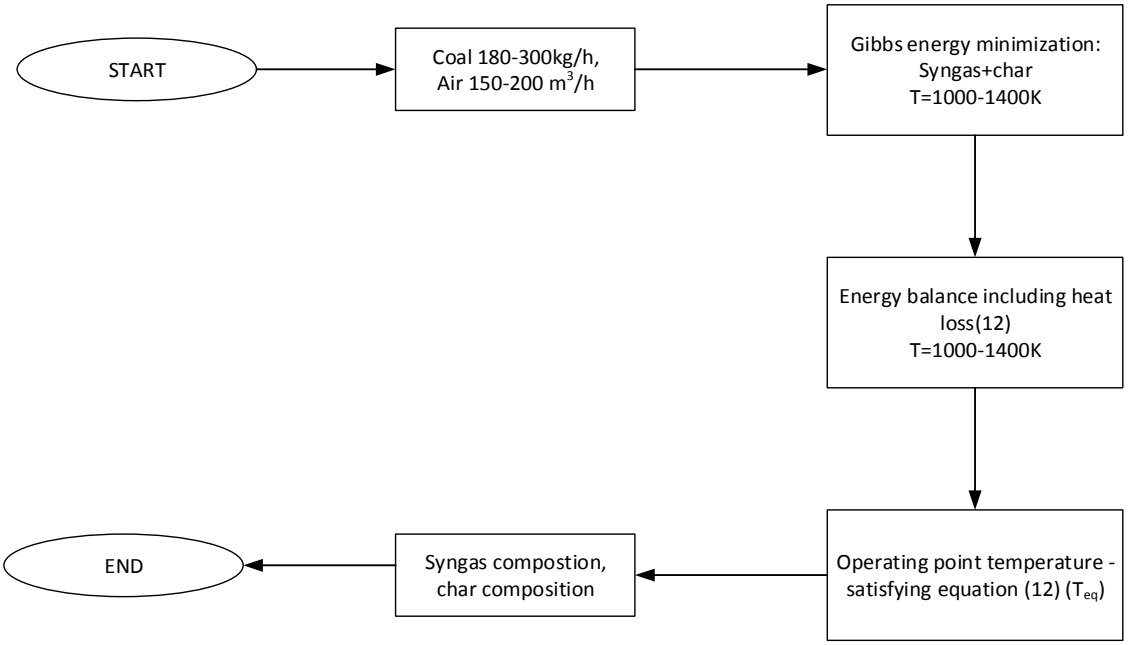


Fig. 3. Computational algorithm

The model presented above incorporates both exothermic combustion and endothermic gasification reactions, without defining them explicitly. The results of the reactions are presented in terms of the final gas composition at a given temperature and overall enthalpy of the process. Calculations of the quasi-equilibrium composition are based on known thermodynamic data for each substance present in the system as well as the mass and energy balance for all flows. The computational algorithm was implemented in a Mathcad 15 (Mathcad, 2001) environment.

The first simulations were based on a purely thermodynamic model, minimizing the total Gibbs energy with five constraining equations representing mass balance. The results of this simulation are presented in Fig. 4. As can be observed, the thermodynamic approach gives very inaccurate results, showing a tendency to overestimate significantly the yield of hydrogen, carbon monoxide, methane and char, while underestimating the yields of hydrogen and carbon dioxide. The thermodynamic model is also very unstable, producing results which vary by as much as 50–60% in the case of hydrogen. All this makes this model useless in practical applications for fluid bed gasification. To make some necessary

improvements to the model, an insight into the chemistry of the process is needed. Table 4 summarises the main chemical reactions occurring in the gasification process and their equilibrium constants at 1200 K. It was shown by (Ściążko, 2013) that the quasi-equilibrium constant for the Boudouard reaction calculated using experimental results differs substantially from the value calculated from thermodynamic tables. The main reason why the purely thermodynamic model fails to predict the correct composition of gasification products is that it does not include the kinetic effects of chemical reactions occurring during gasification process. Hence, to improve the accuracy of the thermodynamic model, certain correction factors, based on analysis of the differences in the equilibrium constants, were introduced, creating a quasi-thermodynamic-empirical model.

Table 4. List of main gasification reactions with their enthalpies (Higman, 2003) and equilibrium constants

| | Reaction | $\Delta_r H$ (MJ/kmol) | $K_{eq}$ (1200 K) |
|---|---|---|---|
| 4.1 | $C + O_2 \rightarrow CO_2$ | -384 ±0.13 | $1.808\times10^{17}$ |
| 4.2 | $H_2 + ½\ O_2 \rightarrow H_2O$ | -242 ±0.04 | $3.027\times10^{9}$ |
| 4.3 | $C + CO_2 \rightarrow 2CO$ | +172 ±0.47 | 56.90 |
| 4.4 | $C + H_2O \rightarrow CO + H_2$ | +131 ±0.21 | 37.57 |
| 4.5 | $CO + H_2O \rightarrow CO_2 + H_2$ | -41 ±0.34 | 0.61 |

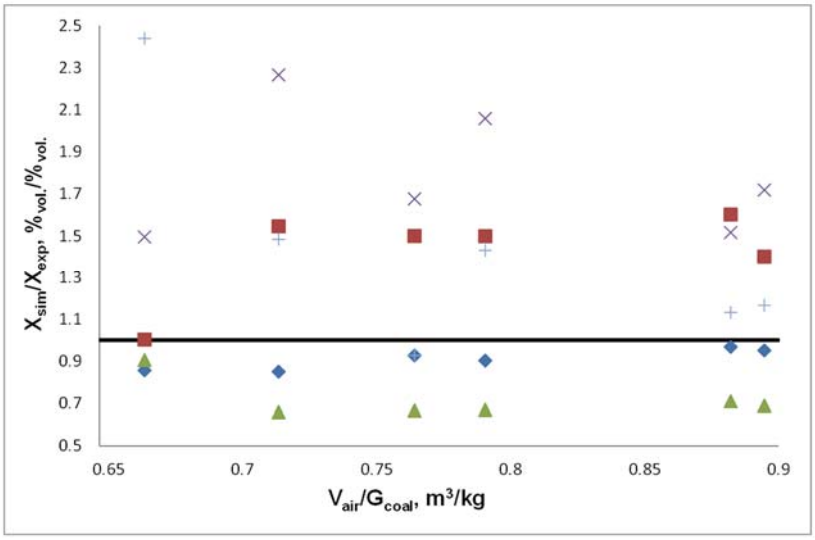


Fig. 4. Syngas composition and char yield for a purely thermodynamic model
(♦ - $N_2$, ■ – CO, ▲ – $CO_2$, × - $H_2$, + - $CH_4$)

Using experimental concentrations of carbon monoxide and carbon dioxide, the ratio of the experimental and thermodynamic equilibrium constants was calculated. The quasi-equilibrium state of the Boudouard reaction is simulated by Eq. (20). The correction function $\alpha(T)$ in Eq. (21) was calculated by means of regression analysis of a series of experimental results.

$$\frac{[CO]^2}{[CO_2]} = \alpha(T) e^{\frac{-\Delta_r G}{RT}} \tag{20}$$

$$\alpha(T) = e^{-0.005786\ T} \tag{21}$$

Eqs. (20-21) were added to the Mathcad solve block as additional constraining equations. The correction made it possible to decrease the error of simulation to below 25% (Fig. 5), which is a much

better result than the approximately 60% error with respect to carbon monoxide yield obtained from the purely thermodynamic model. On the other hand, introducing this correction doubled the error for hydrogen yield, which was greatly overestimated (by up to 600%), making it necessary to improve the model's performance with respect to hydrogen yield.

Consequently, another correction was introduced with respect to the water gas shift reaction (22). Starting from the thermodynamic equilibrium constant for the water gas shift reaction and with the help of experimental results and error minimisation method, a correction function was obtained and introduced as another constraining equation in the following form:

$$\frac{[CO_2][H_2]}{[CO][H_2O]} = \gamma\, e^{\frac{-\Delta G_{wgs}}{RT}} \tag{22}$$

where γ is a constant correction factor, obtained in a statistical analysis to minimise simulation error. For the best fit of the simulation to the experimental results the value $\gamma$=2 was obtained, suggesting that hydrogen is formed faster than the thermodynamic predictions for the water gas shift reaction. This is also a much higher value than that discussed by (Ściążko and Stępień, 2014). In that paper a limited number of components was taken into account which resulted in different percent fractions of considered species, than in the present work. Explanation of this phenomenon can be found in the combined effect of heterogeneous $C + H_2O \rightarrow CO + H_2$ and homogeneous $CO + H_2O \rightarrow CO_2 + H_2$ reactions, but most probably in the effect of pyrolysis gas released from coal at the early stage of gasification.

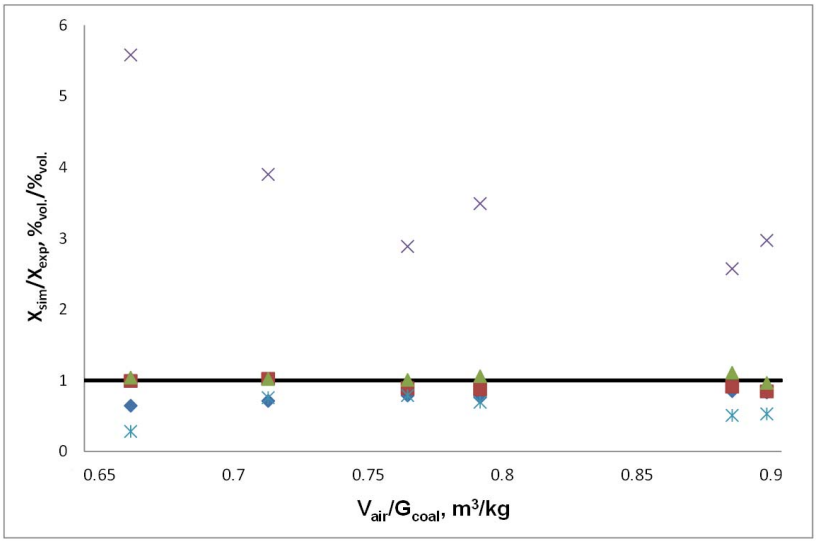


Fig. 5. Syngas composition ratio with quasi-equilibrium Boudouard reaction correction
(♦ - $N_2$, ■ – CO, ▲ – $CO_2$, × - $H_2$, + - $CH_4$)

As previously mentioned, it is assumed that light hydrocarbons and tar in the gasification process are formed not as a result of an equilibrium-governed reaction, but during pyrolysis, which is the first step of coal gasification. In the model the formation of hydrocarbons – propane (Eq. (23)) and benzene (Eq. (24)) – was governed by empirically obtained correlations with gasification temperature. Values obtained from the following functions represent the yields of hydrocarbons, kmol/h.

$$n_{C_3H_8}(T) = 1.734 \times 10^{-4} T - 0.04 \tag{23}$$

$$n_{C_6H_6}(T) = 7.587 \times 10^{-5} T - 0.017 \tag{24}$$

Tar, represented by naphthalene, was calculated parametrically based on the amount of gas produced. The value represents averaged experimental data and was considered to be constant and equal to 0.01 kg/Nm$^3$.

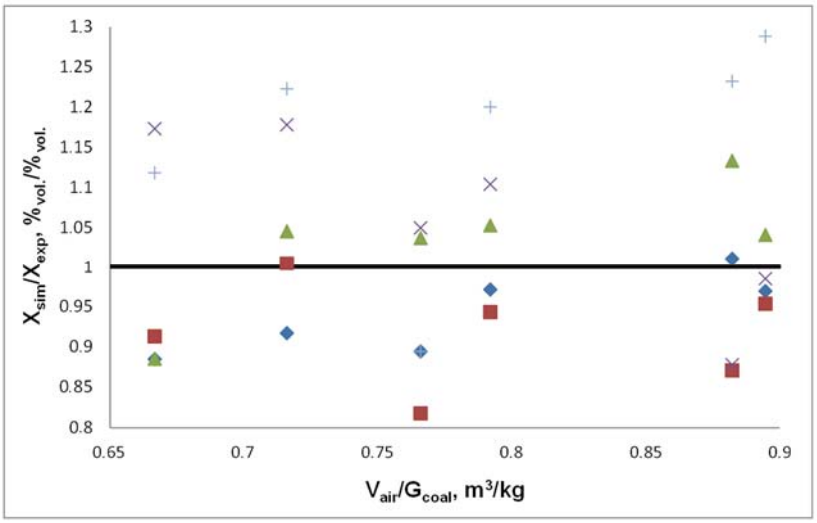


Fig. 6. Comparison of experimental data with simulation results for different air-to-coal ratios (♦ - $N_2$, ■ – CO, ▲ – $CO_2$, × - $H_2$, + - $CH_4$)

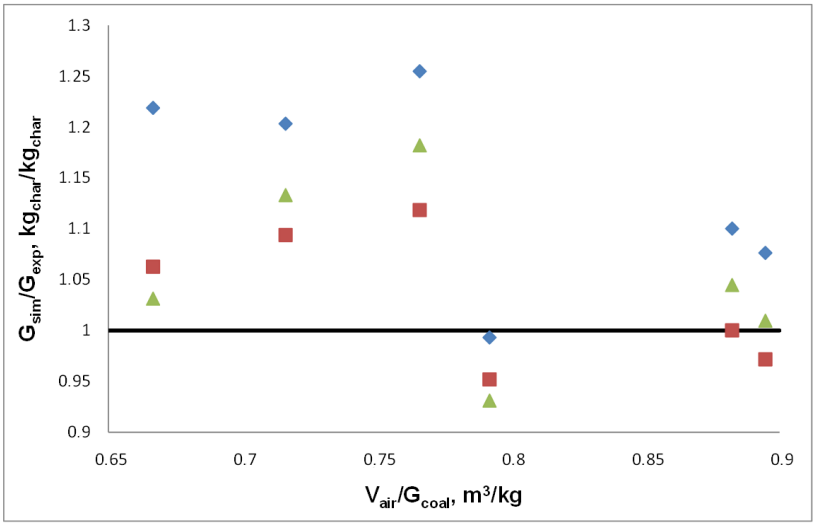


Fig. 7. Char yield for the thermodynamic model (♦), modified Boudouard reaction (▲), and hybrid model (■)

The performance of the final model after these two corrections is shown in Fig. 6. For clarity purposeses, this model is further called the "hybrid model". As can be seen, the simulation error decreased significantly and is at an acceptable level of approximately 20% with respect to most gaseous components. The only exception is methane, which is overestimated by as much as 30% for higher air-to-coal ratios. However, methane content was never higher than 5%. The above mentioned corrections might be regarded as a projection of the real behaviour of the reaction system, taking into account a thermodynamic equilibrium model modified with the kinetic restrictions typical of fluid bed gasifiers. The results imply that kinetic effects play a major role in the fluid bed gasification process. For example,a comparison of the theoretical value of the equilibrium constant for the heterogeneous Boudouard reaction (4.3) given in Table 4 with that obtained by incorporating Eqs. (20-21), which give the quasi-equilibrium constant $K_{qB}(1200) = 0.111$, clearly shows discretisation of the equilibrium state by the kinetics of the process. This phenomenon is less visible in the homogeneous water gas shift

reaction, which is not only closer to its equilibrium state but even higher due to the combined effect of heterogeneous and homogeneous steam reactions.

Figure 7 presents char yield for the three versions of the model. The thermodynamic model shows a tendency to overestimate the yield of char by up to 25%. After introducing the corrections, the overestimation decreases to no more than 10%. Figure 8 presents a comparison of gasification temperature for the developed models. The temperatures calculated from both the thermodynamic and the final hybrid model are in good agreement with those measured in experimental tests. However, introducing only Boudourd reaction correction caused a significant reduction in the calculated quasi-equilibrium temperature.

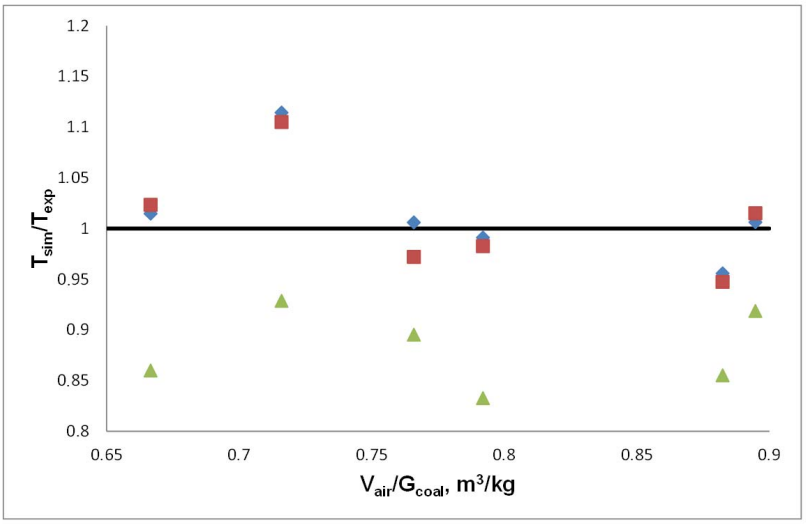


Fig. 8. Quasi-equilibrium state temperature for the thermodynamic model (♦), modified Boudouard reaction (▲), and hybrid model (■)

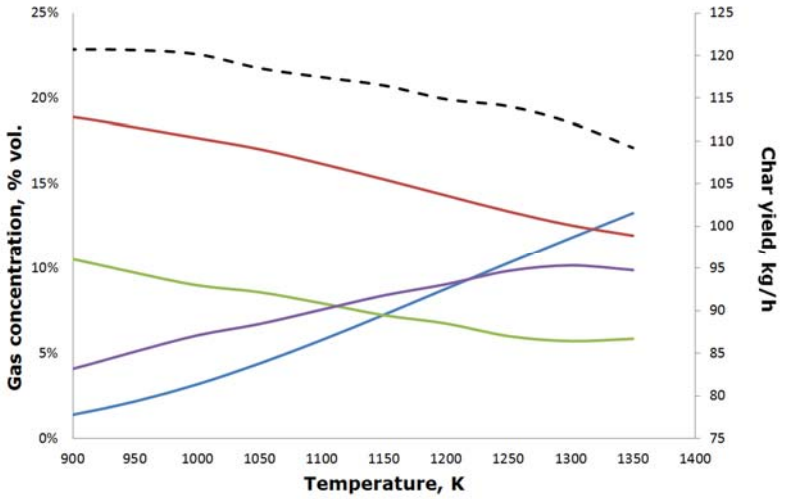


Fig. 9. Model prediction - syngas composition vs. temperature for air/coal=1m$^3$/kg (CO-blue, $CO_2$-red, $CH_4$-green, $H_2$-violet, char-black).

Figure 9 presents model performance in predicting gas composition and char yield depending on the temperature of the process. Calculations were performed assuming the inlet stream of coal $m_{coal}$=250 kg/h and the inlet stream of air $V_{air}$=250 m$^3$/h. As can be seen increasing temperature causes a decrease in char yield as well as carbon dioxide and methane. On the other hand, an increase in the yields of carbon monoxide and hydrogen are observed. Another important observation is that the

equilibrium temperature between CO and $CO_2$ ($CO/CO_2$=1) is by approximately 300K higher than the theoretical one (Reed T., 2006).

## 4. CONCLUSIONS

The free Gibbs energy minimisation method, which is convenient in the analysis of complex processes like gasification, was used to model the process. The model predicts the formation of the eight key gaseous species CO, $CO_2$, $H_2O$, $H_2$, $H_2S$, $N_2$, COS and $CH_4$, volatile hydrocarbons represented by propane and benzene, tar represented by naphthalene, and char containing the five elements C, H, O, N, S and inorganic matter. The molar fractions of gaseous species were taken into account for equilibrium calculations, as well as the mixing effect in the case of light hydrocarbons and tar.

For better accuracy, the basic thermodynamic model was improved by adding certain correction factors reflecting real, quasi-equilibrium states for two selected but leading reactions, i.e. the water gas shift and Boudouard reactions.

The final model resulted in a simulation error not greater than 20% with respect to most gaseous components. The only exception is methane, which is overestimated by as much as 30% for higher air-to-coal ratios. However, methane content was never higher than 5%.

The corrections might be regarded as a projection of the real behaviour of the reaction system, taking into account a thermodynamic equilibrium model modified with the kinetic restrictions typical of fluid bed gasifiers.

*The work was conducted within the framework of the strategic project no. SP/E/3/77008/10, financed by the National Centre for Research and Development*

## SYMBOLS

| | |
|---|---|
| $\theta$ | oxygen content, % |
| $\delta$ | relative mass balance error, % |
| $\Delta G$ | molar free Gibbs energy, kJ/kmol |
| $\Delta H$ | molar enthalpy, kJ/kmol |
| $\Delta S$ | molar entropy, kJ/kmol |
| $\Delta h$ | total enthalpy of stream, kJ |
| $A$ | ash content. % |
| $C$ | carbon content, % |
| $H$ | hydrogen content, % |
| $S$ | sulphur content, % |
| $C_p$ | heat capacity, J/(mol·K) |
| $n$ | number of moles |
| $R$ | universal gas constant J/(mol·K) |
| $T$ | temperature, K |
| $Q$ | heat loss, kJ |
| $V$ | volume stream, $m^3/h$ |
| $G$ | mass stream, kg/h |

*Superscripts*

| | |
|---|---|
| *daf* | dry and ash free |

| | |
|---|---|
| *ar* | as received |
| *a* | analytical |
| *0* | standard reference condition |
| *l* | liquid |

*Subscripts*

| | |
|---|---|
| *i* | i-th component |
| *f* | formation |
| *c* | combustion |
| $C_nH_m$ | hydrocarbons $C_2H_4$-$C_3H_8$ |
| *sim* | simulation |
| *exp* | experimental |
| *r* | reaction |
| *solid* | coal or char |

## REFERENCES

Chen C.J., Hung C.I., Chen W.H., 2012. Numerical investigation on performance of coal gasification under various injection patterns in an entrained flow gasifier. *Appl. Energy*, 100, 218-228. DOI: 10.1016/j.apenergy.2012.05.013.

Esmaili E., Mahinpey N., Lim Jim C., 2013. Modified equilibrium modelling of coal gasification with in situ $CO_2$ capture using sorbent CaO: Assessment of approach temperature. *Chem. Eng. Res. Des.*, 1361-1369. DOI: 10.1016/j.cherd.2013.02.015.

Florin N.H., Harris A.T., 2007. Hydrogen production from biomass coupled with carbon dioxide capture: The implications of thermodynamic equilibrium. *Int. J. of Hydrog. Energy*, 32**,** 4119-4134. DOI: 10.1016/j.ijhydene.2007.06.016.

Higman Ch., van der Burgt M., 2003. *Gasification,* Elsevier.

Irfan M.F., 2011. Coal gasification in $CO_2$ atmosphere and its kinetics since 1948: A brief review. *Energy*, 36, 12-40. DOI: 10.1016/j.energy.2010.10.034.

Jarungthammachote S., Dutta A., 2008. Equilibrium modelling of gasification: Gibbs free energy minimisation approach and its application to spouted bed and spout-fluid bed gasifiers. *Energy Convers. Manag*., 49, 1345-1356. DOI: 10.1016/j.enconman.2008.01.006.

Kaiho M., Yamada O., 2012. Stoichiometric approach to the analysis of coal gasification process, In: Innocenti A. (Ed.), *Stoichiometry and materials science - When numbers matter.* InTech. DOI: 10.5772/37809.

Kangas P., Hannula I., Koukkari P., Hupa M., 2014. Modelling super-equilibrium in biomass gasification with the constrained Gibbs energy method. *Fuel*, 129, 86-94, DOI: 10.1016/j.fuel.2014.03.034.

Li X., Grace J.R., Watkinson A.P., Lim C.J., Ergüdenler A., 2001. Equilibrium modelling of gasification: A free energy minimisation approach and its application to a circulating fluidized bed coal gasifier. *Fuel*, 80, 195-207. DOI: 10.1016/S0016-2361(00)00074-0.

Mann M.D., Knutson R.Z., Erjavec J., Jacobsen J.P., 2004. Modelling reaction kinetics of steam gasification for a transport gasifier. *Fuel*, 83, 1643-1650. DOI: 10.1016/S0016-2361(00)00074-0.

*Mathcad user's guide with reference manual,* 2001. MathSoft Engineering & Education, Inc. USA.

Miao Qi, Zhu Jesse, Barghi S., Wu Chuangzhi, Yin Xiuli, Zhou Zhaoqiu, 2014. Modelling biomass gasification in circulating fluid beds, *Renewable Energy*, 50, 655-661. DOI: 10.1016/j.renene.2012.08.020.

Neron A., Lantagne G., Marcos B., 2012. Computation of complex and constrained equilibria by minimisation of the Gibbs free energy. *Chem. Eng. Sci.,* 82, 260-271. DOI: 10.1016/j.ces.2012.07.041.

Pengmei Lv., Yuan Zhenhong, Ma Longlong, Wu Chuangzhi, Chen Yong, Zhu Jingxu, 2007. Hydrogen-rich gas production from biomass air and oxygen/steam gasification in a downdraft gasifier. *Renewable Energy*, 32, 2173-2185. DOI: 10.1016/j.renene.2006.11.010.

M.S. Rao Singh S.P., Sodha S.P., Dubey A.K., Shyam M., 2004. Stoichiometric, mass, energy and exergy balance analysis of countercurrent fixed-bed gasification of post-consumer residues. *Biomass Bioenergy*, 27, 155-171. DOI: 10.1016/j.biombioe.2003.11.003.

Reed T., 2006. *The Boudouard equation: Chart and spreadsheet*. BioEnergy lists: Gasifiers & gasification. Retrived 25 March 2015, from: http://gasifiers.bioenergylists.org/reedboudouard.

Ściążko M., Stępień L., 2014. Termodynamiczno-empiryczny model powietrznego zgazowania węgla. *Przem. Chem.*, 93, 368. DOI: 10.12916/przemchem.2014.368.

Silaen A., Wang T., 2010. Investigation of the coal gasification process under various operating conditions inside a two stage entrained flow gasifier. *Proceedings of the 27th Pittsburgh Coal Conference*. Istanbul, Turkey, 11-14 October 2010.

Shabbar S., Janajreh I., 2013. Thermodynamic equilibrium analysis of coal gasification using Gibbs energy minimisation method. *Energy Convers. Manage*., 65, 755-763. DOI: 10.1016/j.enconman.2012.02.032.

Szarawara J., 2007. *Termodynamika chemiczna stosowana*, WNT.

Ściążko M., 2013. Rank-dependent formation enthalpy of coal. *Fuel*, 114, 2-9. DOI: 10.1016/j.fuel.2012.06.099.

Thanh D.B. Nguyen Lim, Young-Il, Song Byung-Ho, Kim Si-Moon, Joo Yong-Jim, Ahn Dal-Hong, 2010. Two-stage equilibrium model applicable to the wide range of operating conditions in entrained-flow coal gasifiers. *Fuel*, 89, 3901-3910. DOI: 10.1016/j.fuel.2010.06.044.

Tremel A., Spliethoff H., 2013. Gasification kinetics during entrained flow gasification – Part III: Modelling and optimisation of entrained flow gasifiers. *Fuel*, 107, 170-182. DOI: 10.1016/j.fuel.2013.01.062.

Yoshida H., Kiyono F., Tajima H., Yamasaki A., Ogasawara K., Masuyama T., 2008. Two-stage equilibrium model for a coal gasifier to predict the accurate carbon conversion in hydrogen production. *Fue*l, 87, 2186-2193. DOI: 10.1016/j.fuel.2008.01.009.

*Received 23 December 2014*
*Received in revised form 19 February 2015*
*Accepted 25 February 2015*

## APPENDIX

Table A. Heat capacity coefficients according to (Szarawara, 2007)

| | *a* | *b* | *c* | *d* | *e* |
|---|---|---|---|---|---|
| C | 17.16 | 4.27 | 0 | -8.79 | 0 |
| $H_2$ | 29.10 | -1.92 | 4.00 | 0 | -0.87 |
| $O_2$ | 36.18 | 0.85 | 0 | -4.31 | 0 |
| $N_2$ | 28.90 | -1.57 | 8.08 | 0 | 2.85 |
| S | 14.99 | 26.12 | 0 | 0 | 0 |
| $SO_2$ | 25.77 | 57.93 | -38.10 | 0 | 8.61 |
| CO | 28.15 | 1.67 | 5.37 | 0 | -2.22 |
| $CO_2$ | 22.25 | 59.8 | -35.00 | 0 | 7.47 |
| $H_2O^{(l)}$ | 75.33 | 0 | 0 | 0 | 0 |
| $H_2O^{(g)}$ | 32.23 | 1.92 | 10.55 | 0 | -3.59 |
| $H_2S$ | 29.59 | 13.09 | 5.71 | 0 | -3.29 |
| NO | 27.05 | 9.87 | -3.23 | 0 | 0.36 |
| $NO_2$ | 22.94 | 57.14 | -35.2 | 0 | 7.87 |
| $CH_4$ | 19.88 | 50.23 | 12.68 | 0 | -11.01 |
| $C_2H_6$ | 6.90 | 172.63 | -64.05 | 0 | 7.28 |
| $C_3H_8$ | -4.04 | 304.70 | -157.18 | 0 | 31.73 |
| COS | 47.43 | 9.12 | 0 | -9.04 | 0 |
| $SiO_2$ | 46.97 | 34.32 | 0 | -11.3 | 0 |
| $C_6H_6$ | -36.21 | 484.65 | -315.62 | 0 | 77.61 |
| $C_{10}H_8$ | 0 | 539.80 | 200.00 | 0 | 20.00 |